Photorecombination of C^{4+} ions in low-lying resonance energy regions

Li-Bo Zhao, Akira Ichihara, and Toshizo Shirai
Japan Atomic Energy Research Institute, Tokai-mura, Ibaraki 319-1195, Japan
(Received 28 January 2000; published 14 July 2000)

Within the framework of the rigorous continuum-bound transition theory of Davies and Seaton [J. Phys. B **2**, 757 (1969)], we have developed a numerical method to calculate low-lying resonance photorecombination by directly evaluating the Cauchy principal value of the integral in scattering matrices. The required dipole matrix was obtained using the close-coupling *R*-matrix code. The advantage of this method is that radiation damping can be accurately estimated and it can naturally be applied to stronger resonance-resonance interference systems. On the basis of this scheme, photorecombination cross sections of C^{4+} ions in the *KLL*, *KLM*; and *KLN* resonance energy regions were calculated, and compared with synchrotron storage ring experimental data and perturbative and close-coupling theoretical results. The comparisons showed that our damped cross sections reproduce the results of the high-resolution experimental measurements, and are in agreement with the theoretical calculations. However, our undamped cross sections are larger than the close-coupling results in the parametrized method by a factor of up to 3. The discrepancies were interpreted.

PACS number(s): 34.80.Kw

I. INTRODUCTION

Photorecombination is conventionally regarded as proceeding via two dominant channels, radiative recombination (RR) and dielectronic recombination (DR). RR is a direct transition from a free to a bound state with the emission of a photon, whereas DR is an indirect two-step process in which a free electron is captured into a doubly excited state followed by a stabilizing radiative transition. From the point of view of quantum mechanics, there exists interference between the two channels if the RR and DR have the same initial and final states. The interference term is also a contributor. Photorecombination is an atomic process of interest in applied and fundamental physics [1]. This process may seriously affect the ionization balance and ionic excited-state distributions of laboratory and astronomical plasmas, as in fusion devices and in the solar corona, and is an important cooling mechanism of high-temperature plasmas [2,3]. Dielectronic satellites produced in photorecombination are also used as diagnostics of plasma densities and electron temperatures [4]. On the other hand, investigation of photorecombination is an efficient means to study electron correlation, effects of relativity and QED, radiation damping [5], and quantum-mechanical interference effects between the DR resonances and the RR background. Since the doubly excited states involved in dielectronic recombination are strongly correlated systems, theories characterizing electron correlation are easily examined by comparison with experiments. The energy levels and the shapes of the observed resonance structures can feed back information on relativistic and QED corrections to electron-electron interaction and radiation damping. With increase of the effective atomic number, the interference between DR and RR in photorecombination becomes more and more striking. Thus observation of the interference becomes practicable. By investigating photorecombination of ions, information about many fundamental physical effects can be extracted. Meanwhile, good understanding of these effects is of importance to practical applications.

A great deal of progress has been made in studies on photorecombination of ions with free electrons [6–15]. In particular, the DR-RR interference in highly charged uranium ions has been observed at the super-EBIT facility of the Lawrence Livermore National Laboratory [16]. Radiation damping was studied, and turned out to be important [17,18]. However, there are still some experiments that cannot be interpreted by existing theory. The double-peak structures of resonances for several kinds of He-like ions, C^{4+}, N^{5+}, O^{6+}, and F^{5+}, were not reproduced by calculations using perturbative theory [13,14,19–21]. Badnell, Pindzola, and Griffin [20] performed a simplified model calculation and obtained the double-peak structure for DR of O^{6+} ions, but they thought a close-coupling calculation would be required to explain the experimental features. In merged-beam experiments and ion storage ring experiments with several kinds of ions, very strong increases of the measured rates were seen over the calculated rates by factors of up to 4–10 [22–24]. Schippers *et al.* [25] experimentally searched for asymmetric line shapes, as predicted by the theories [26], due to DR-RR interference for Ar-like Sc^{3+} and Ti^{4+}. However, the measurements are in disagreement with the calculations within the experimental uncertainty. A conclusive statement could not be made about whether, in the energy range 12.2–18.2 eV, asymmetric line shapes for Sc^{3+} are present because of the lack of statistics. But recently [27], these authors attributed the discrepancies to the difficulties in describing many-electron-atom systems correctly. Concerning radiation damping, there are two different views. Pradhan and Zhang [10] thought that radiation damping is important only for highly charged H- and He-like ions. Badnell, Gorczyca, and Price [18] studied the effects of radiation damping on low-lying photorecombination resonances for H-like through Ni-like ions, and concluded that it is not safe to assume that radiation damping can be neglected for astrophysical ions, even after excluding the cases of H- and He-like ions. Their undamped cross sections for the *KLN* resonance of C^{4+} ions differ by a factor of up to 1 in the peak position [18].

Theoretically there are two ways to investigate photore-

combination, perturbative and nonperturbative approaches. The perturbative methods generally adopt the independent-process and isolated-resonance approximations (e.g., see [1,11,28]). That means that the effects of the resonance-resonance and resonance-background interferences are omitted [29]. The advantage of using perturbative theory is that either inclusion or exclusion of radiation damping is straightforward, and this class of theories can also be applied to studies of interference, for example, the third-order perturbative study of Pindzola *et al.* [30]. But obviously it is impracticable to include all the perturbative orders. Nonperturbative approaches, such as the close-coupling *R*-matrix theories of Burke, Hibbert, and Robb [31], can automatically involve all orders of the interference. Based on the *R*-matrix theory, Robicheaux *et al.* [9] developed a radiative optical-potential method. This method proved to be very successful in calculating photorecombination cross sections [17,29]. Also, Nahar and Pradhan [8] extended the close-coupling *R*-matrix theory to photorecombination, but their treatment did not take effects of radiation damping into account. The prescription not to include radiation damping, which is called the inverse-photoionization method, works well for low-charged ions, since radiative rates scale as the effective charge $Z_{\rm eff}^4$. The radiative width for ions with small $Z_{\rm eff}$ is much smaller than the autoionization width. However, with increase of $Z_{\rm eff}$, the effects of radiation damping on resonance structures grow larger. The neglect of radiative widths leads to a severe underestimate of the total width, and therefore a corresponding overestimate of DR cross sections, as pointed out by Gorczyca *et al.* [29]. Based on Davies and Seaton's theory [5] for including radiation damping, Sakimoto, Terao, and Berrington [32] developed a numerical scheme to evaluate photorecombination and photoionization. Further approximations were made in their calculations of dipole matrix elements. First the dipole matrices were parametrized and analytically continued into complex planes. Then the necessary contour integral was evaluated, and finally the scattering matrix was obtained. Pradhan and Zhang [10] applied this scheme to the evaluation of photorecombination of ions in the energy region related to low-lying resonances. The drawback of this scheme is that the overlapping of resonances was not well treated. Recent research on electron-impact excitation in Mg-like ions indicated that huge enhancements in the resonance line shapes occur due to direct configuration mixing between the two resonance states; however, interference through a continuum state does not result in this kind of enhancement [33]. It is obvious that an efficient treatment of interference is inevitable. Sakimoto [34] further dealt with photorecombination of overlapping resonances, but the overlap was restricted to that from radiative decay effects, due to difficulties of fitting the overlapping resonances from autoionization effects.

In this paper, we develop a numerical method to evaluate photorecombination of ions in low-lying resonance energy regions. Our method is based on the rigorous continuum-bound transition theory of Davies and Seaton, and no approximation is made. Using this method, we investigated photorecombination of C^{4+} ions for the *KLL*, *KLM*, and *KLN* resonances. In the second section, we will outline Davies and Seaton's continuum-bound transition theory, and the perturbative theory to calculate photorecombination cross sections for comparison. In the third section, the calculated results of photorecombination cross sections are given, and the effects of radiation damping on these resonances are discussed. The final section summarizes our conclusions.

II. THEORETICAL METHODS

A. The rigorous theory of continuum-bound transitions

Davies and Seaton's [5] theory treated photorecombination in a unified manner, including radiative and dielectronic recombination and their interference. This theory starts from neglecting the interaction with radiation fields, and assumes that the electron-ion systems can be exactly solved. The solution of the wave functions is used to provide a representation to set up equations including interaction with radiation fields. In the interaction Hamiltonian, only the electric-dipole terms are retained, and the radiation field is restricted to considering only the states with no photon and with one photon. The resulting time-dependent matrix equations for the probability amplitudes are solved by application of the Laplace transform. The solutions for the probability amplitudes can be expressed in terms of a scattering matrix $\mathcal{S}$ with partitioning

$$\mathcal{S}=\begin{pmatrix} \mathcal{S}_{ee} & \mathcal{S}_{ep} \\ \mathcal{S}_{pe} & \mathcal{S}_{pp} \end{pmatrix}, \tag{1}$$

where $\mathcal{S}_{ee}$ represents the submatrix for electron-electron scattering allowing for radiative decays, $\mathcal{S}_{ep}$ that for photoionization, $\mathcal{S}_{pe}$ that for photorecombination, and $\mathcal{S}_{pp}$ that for photon-photon scattering. The submatrices $\mathcal{S}_{ee}$ and $\mathcal{S}_{pe}$ are written, respectively, in the forms

$$\mathcal{S}_{ee}=\mathbf{S}[1-2\pi^2\mathbf{D}(1+\mathbf{Z})^{-1}\mathbf{D}^\dagger], \tag{2}$$

$$\mathcal{S}_{pe}=-2\pi i(1+\mathbf{Z})^{-1}\mathbf{D}^\dagger, \tag{3}$$

where **S** is the electron-electron scattering matrix neglecting radiative channels, **D** is the reduced dipole matrix with its matrix element defined as

$$\mathbf{D}_{\gamma J,\gamma' J'}=\left(\frac{2\omega^3\alpha^3}{3\pi}\right)^{1/2}\frac{\langle \gamma J\|\mathbf{R}\|\gamma' J'\rangle}{(2J+1)^{1/2}}, \tag{4}$$

and the matrix **Z** is related to interaction with the radiation field, given by

$$\mathbf{Z}(\Omega)=-i\pi\int dE\,\frac{D^\dagger(E)D(E)}{E-\Omega-i\epsilon}. \tag{5}$$

Equation (5) can be further written as

$$\mathbf{Z}(\Omega)=\pi^2\mathbf{D}^\dagger(\Omega)\mathbf{D}(\Omega)-i\pi\mathcal{P}\int dE\,\frac{\mathbf{D}^\dagger(E)\mathbf{D}(E)}{(E-\Omega)}. \tag{6}$$

In Eqs. (4), (5), and (6), α is the fine-structure constant, ω is the photon energy in units of hartrees, $\mathbf{R}=\Sigma_i\mathbf{r}_i$ is the dipole operator, in which the summation is over all atomic elec-

trons, γJ and $\gamma' J'$, respectively, specify the continuum and bound states of the atomic system, and J (J') are the total angular momenta, the wave function of the continuum electron is normalized per hartree and $\mathcal{P}$ means the Cauchy principal value of the integral.

If only the first-order term of **D** is retained, Eqs. (2) and (3) are approximated as

$$\mathcal{S}_{ee} = \mathbf{S}, \tag{7}$$

$$\mathcal{S}_{pe} = -2\pi i \mathbf{D}^{\dagger}. \tag{8}$$

Equations (7) and (8) are the expressions for $\mathcal{S}_{ee}$ and $\mathcal{S}_{pe}$ without radiation damping.

For a given entrance channel j, the partial probability for photorecombination is

$$\mathsf{P}_j^{\mathrm{PR}} = (1 - \mathcal{S}_{ee}^{\dagger}\mathcal{S}_{ee})_{jj} = (\mathcal{S}_{pe}^{\dagger}\mathcal{S}_{pe})_{jj}. \tag{9}$$

The total cross section for photorecombination can be written as

$$\sigma_{\mathrm{PR}}(E) = \frac{\pi}{2k^2 g} \sum_j g_j \mathsf{P}_j^{\mathrm{PR}}, \tag{10}$$

where k is the wave number of the incident electron, and g and g_j are the statistical weights of the recombining ion state and the continuum state, respectively.

B. The perturbative theory

In theoretical calculations of photorecombination based on the perturbative theory, the independent-process and isolated-resonance approximations are generally utilized. In these approximation, DR cross sections can be written in the form

$$\sigma_d(\epsilon) = \frac{\pi^2}{\epsilon} \frac{g_d}{g_i} \Gamma_a \frac{\Gamma_r}{\Gamma_a + \Gamma_r} L_d(\epsilon), \tag{11}$$

where ϵ denotes the free-electron energy in rydbergs and g_i and g_d are the statistical weights of the initial ionic core and the doubly excited intermediate state. Γ_a and Γ_r are the autoionization and radiative widths of the intermediate state, defined by

$$\Gamma_a = 2\pi \left| \left\langle \Psi_i \left| \sum_{s<t} \frac{1}{r_{st}} \right| \Psi_d \right\rangle \right|^2, \tag{12}$$

where Ψ_i and Ψ_d are antisymmetrized multielectron wave functions for the initial and intermediate doubly excited states, and the continuum state is normalized per unit energy, and

$$\Gamma_r = \frac{4\omega^3}{3c^3} \left| \left\langle \Psi_d \left| \sum_s \mathbf{r}_s \right| \Psi_f \right\rangle \right|^2 \tag{13}$$

where ω is the photon energy, c the velocity of light, and Ψ_f the wave function for the final state. $\Gamma_r/(\Gamma_a + \Gamma_r)$ in Eq. (11) is the branching ratio, and $L_d(\epsilon)$ is the Lorentzian line profile,

$$L_d(\epsilon) = \frac{(\Gamma_a + \Gamma_r)/2\pi}{(\epsilon - \epsilon_d)^2 + (\Gamma_a + \Gamma_r)^2/4}. \tag{14}$$

If Z_{eff} is small, the radiative width may be omitted. In this case, the total width $\Gamma = \Gamma_a + \Gamma_r$ in the denominator of the Lorentzian line profile is approximated by the autoionization width.

III. CALCULATIONS AND DISCUSSION

From Sec. II, it can be seen that, in order to evaluate photorecombination cross sections, one needs to calculate the integral in Eq. (5) or (6). Sakimoto, Terao, and Berrington [32] introduced a parametrized method to perform photorecombination calculations. First the dipole matrix element is expanded into a summation of the resonance and nonresonance contributions. Substituting the expansion into Eq. (5) and evaluating the integral, the parametrized expression for $Z(\Omega)$ can be obtained. Then the dipole matrix element is evaluated by using the close-coupling R-matrix code, and these parameters are obtained by fitting the dipole matrix element. The drawback of this method is that nonisolated resonances cannot be handled. Sakimoto's later treatment for photorecombination of the resonance-resonance interference was still restricted to overlaps due to radiative decay effects [34]. We carried out a precise calculation of photorecombination by directly evaluating the Cauchy principal value of the integral in Eq. (6). This scheme is valid for low-lying resonances, and can be conveniently applied to investigation of the effects of resonance interference. Here recombination cross sections for C^{4+} ions are reported in energy regions related to the *KLL*, *KLM*, and *KLN* resonances. We employed the close-coupling R-matrix approach [31,35] in the *LS* coupling scheme to calculate the dipole matrix elements. The details of R-matrix theory can be found in Refs. [31] and [35], and therefore are not repeated in this report.

The computation carried out in this study starts from the determination of the target states. The 11 lowest target states ($1\ ^1S$, $2\ ^3S$, $2\ ^1S$, $2\ ^3P$, $2\ ^1P$, $3\ ^3S$, $3\ ^1S$, $3\ ^3P$, $3\ ^3D$, $3\ ^1D$, and $3\ ^1P$) are included in our calculations. Hibbert's [36] CIV3 program was used to optimize the $2s$, $2p$, $3s$, $3p$, and $3d$ radial orbitals on the $2\ ^{3,1}S$, $2\ ^{3,1}P$, $3\ ^{3,1}S$, $3\ ^{3,1}P$, and $3\ ^{3,1}D$ states, respectively. The $1s$ orbital is the Hartree-Fock ground-state orbital of C^{4+} of Clementi and Roetii [37]. We calculated the energy levels and the oscillator strengths in the length f_l and velocity f_v forms obtained with our 11-state target wave functions. The evaluated nonrelativistic target terms are in good agreement with observations and with Zhang and Pradhan's calculations [10], and the oscillator strengths in the two forms are well consistent. For instance, for the transition $1s^2\ ^1S - 1s2p\ ^1P$, $f_l = 0.6872$ and $f_v = 0.6835$, and for the transition $1s^2\ ^1S - 1s3p\ ^1P$, $f_l = 0.1674$ and $f_v = 0.1669$. This substantiated the reliability of our target wave functions. These data can be supplied on request.

For each symmetry of the total spin and orbital angular momentum and parity $SL\pi$, R-matrix calculations were performed. In view of the very small contributions to the cross sections from the higher partial waves, only the partial waves

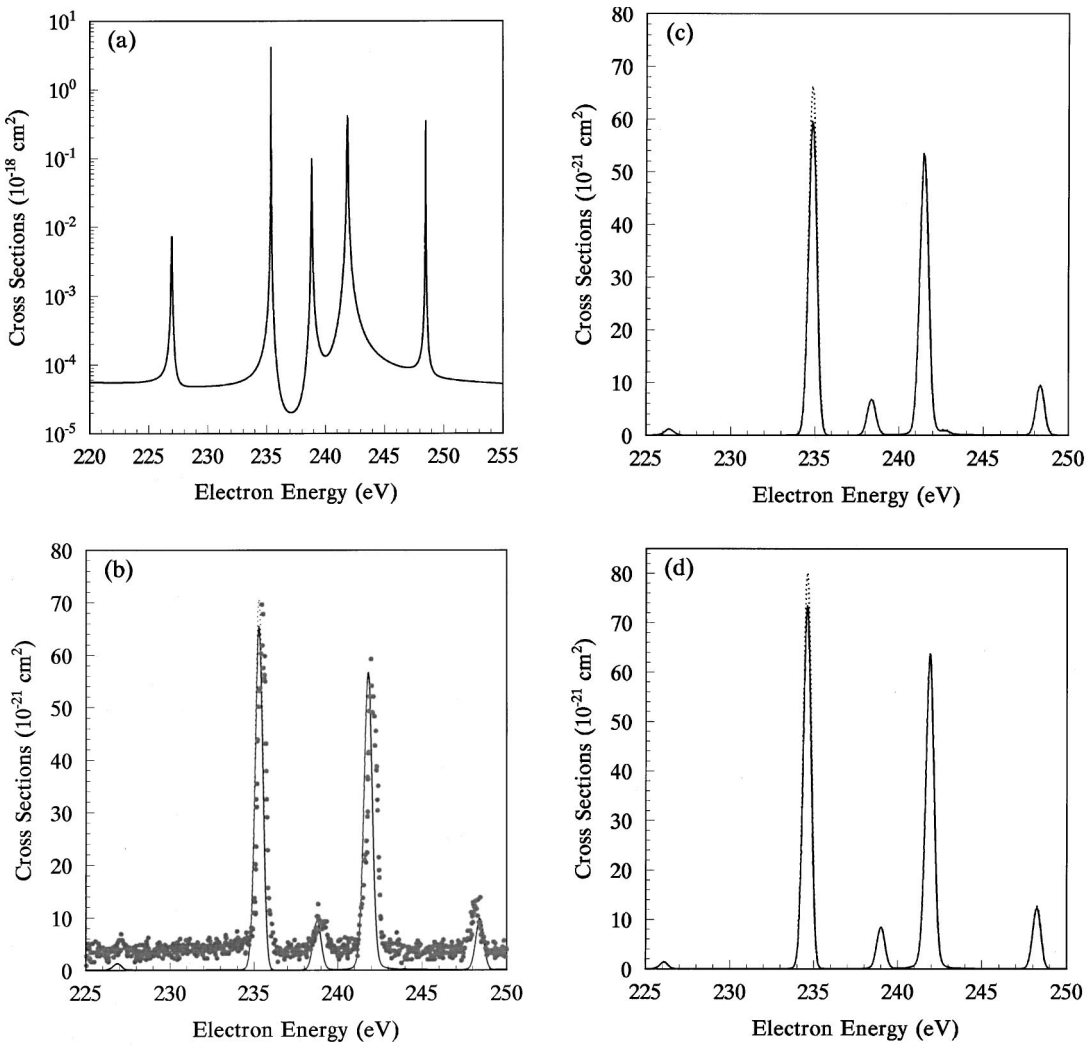

FIG. 1. (a) The photorecombination cross sections for the *KLL* resonance of C^{4+}. (b) Comparisons of the convolved cross sections with the experimental measurement, where the solid and dotted curves, respectively, represent the damped and undamped results calculated on the basis of the rigorous continuum-bound transition theory, whereas the solid dots are the experimental values. (c) The theoretical cross sections with (solid curve) and without (dotted curve) damping from Ref. [10]. (d) The same as in (b), but for the perturbative results.

with $L \leqslant 5$ are retained in our calculations. Furthermore, we adopted a larger-energy-step scan in the background region without resonances than that in the resonance region, since the background varies much smoothly relative to the resonances. This has no influence on the calculation of cross-section convolutions with the experimental electron-energy distribution. But for the resonance states, the large energy step may lead to an underestimate of the cross sections and miss the narrow resonances, owing to the drastic variation of the resonance with energies. To guarantee that each resonance was resolved accurately, we first made a rough energy scan to determine the approximate positions of the resonances. Then, in a small vicinity at each resonance position, a precise step calculation was made until the resonance was absolutely resolved. Figure 1 shows photorecombination cross sections of C^{4+} for the *KLL* resonance as functions of electron energies. In this figure, (a) represents the cross sections with radiation damping, (b) the undamped and damped cross sections in *R*-matrix theory convolved with the experimental electron-energy distributions of Mannervik *et al.* [38], compared with the experimental photorecombination spectra by Mannervik *et al.*, (c) Pradhan and Zhang's theoretical results, and (d) the same as in (b) but calculated in the pertubative theory [39]. In the calculation, we notice that only five of the eight possible resonance states appear. This is due to limitations of the angular momentum and parity conservation in the *LS* coupling scheme. The conservation of total spin angular momentum cuts the two possible quartet states $1s(2p^2\ ^3P)\ ^4P$ and $1s(2s2p\ ^3P)\ ^4P$, and in this region there exists no even-parity continuum state ^2P to interact with the $1s(2p^2\ ^3P)\ ^2P$ resonance. Therefore, dielectronic recombination via the $1s(2p^2\ ^3P)\ ^2P$ resonance is impossible in the *LS* coupling scheme. Only when relativistic effects are taken into account does a very narrow resonance arise. The relativistic calculations of Pradhan and Zhang [10] in the Breit-Pauli approximation displayed such a resonance. However, the resonance is too narrow to be resolved by the experiment [see Fig. 1(b)]. Our cross sections are consistent

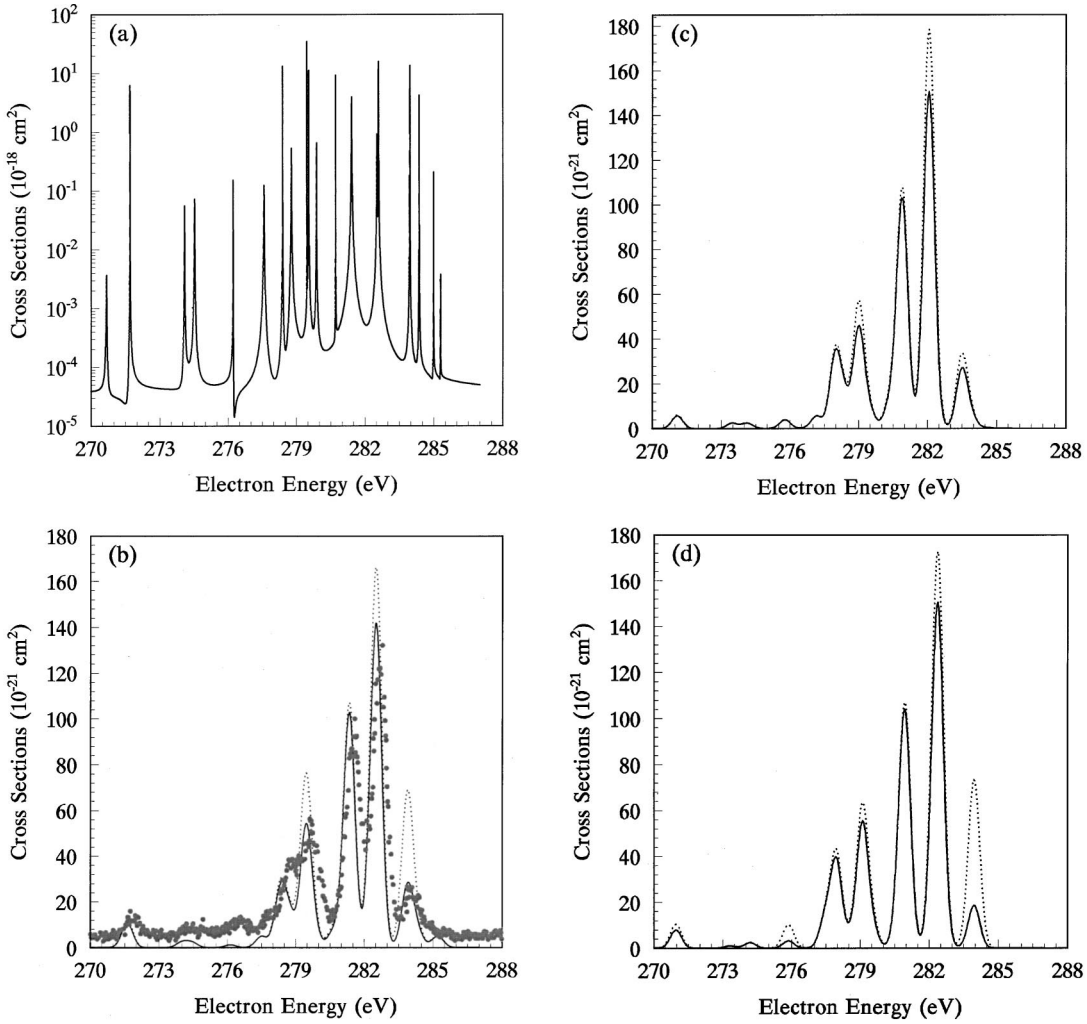

FIG. 2. The same as in Fig. 1, but for the *KLM* resonance.

with Zhang and Pradhan's [10] calculated using the parametrized method of Sakimoto, Terao, and Berrington [32], except for the second resonance $1s(2s2p\ ^3P)\ ^2P$ and the third is $(2s2p\ ^1P)^2P$ (their line is not plotted here). Our peak values are about a factor of 1 and larger than those in the Breit-Pauli approximation in Ref. [10]. The different methods may result in the discrepancies. Moreover, the resonance may be underestimated if the energy steps are not close enough. It should be mentioned that there also exist similar differences in the *KLM* resonances shown in Fig. 2(a). In order to compare with the measurement, the cross sections were convolved with the experimental energy distribution of a pseudo-Maxwellian with vertical temperature $T_\perp$ and longitudinal temperature $T_\parallel$. They are plotted together in Fig. 1(b). $T_\perp$ and $T_\parallel$ are determined from a fitting to the observed $1s2lnl'$ $(n=4-7)$ resonance profiles of the DR resonances [40]. In Ref. [40], DR calculations for these resonances were based on relativistic multichannel theory [12]. The fitting gave $T_\perp=0.08$ eV and $T_\parallel=10^{-4}$ eV. It may be found that the experimental values agree with the present results better than with Pradhan and Zhang's [Fig. 1(c)]. The evaluated cross sections in Ref. [10] were convoluted with a Gaussian distribution of full width at half maximum (FWHM) of 0.57 eV. That means $T_\parallel$ equals about 1.25×10^{-4} eV $[\Delta E(\mathrm{FWHM})=4(\epsilon_d kT_\parallel \ln 2)^{1/2}]$. We tried to employ this $T_\parallel$ value to make the calculation and the differences between our results and theirs were just removed. The autoionization and radiative widths in our perturbative calculations were obtained using Cowan's program [39]. From Figs. 1(b) and 1(d), we see that our perturbative theoretical results agree with that of our close-coupling *R*-matrix approach. Using our code in the Coulomb distorted-wave approximation [41], we also calculated direct radiative recombination to test our *R*-matrix results at energy positions without resonances by comparison. In the calculation, effects of bound $1s$ electrons were taken into account by the rule of Slater screening. To obtain the converged cross section, radiative recombination into $n=2-9$, $0\leqslant l\leqslant n-1$ states was evaluated, where n and l are the principal and angular momentum numbers, respectively. We found agreement between the close-coupling *R*-matrix calculations and the results in the Coulomb distorted-wave approximation. For example, at energies 220, 230, and 240 eV, the cross sections are 42.8, 41.8, and 39.5 b$(10^{-24}\,\mathrm{cm}^2)$, corresponding to 55.5, 55.2, and 48.7 b from the *R*-matrix theory.

The cross sections for the *KLM* resonance are plotted in

Fig. 2. The notation is the same as in Fig. 1. Figure 2(b) shows that our damped *R*-matrix cross sections in the framework of the rigorous continuum-bound transition theory reproduce the high-resolution experimental observations of Mannervik *et al.* [38] and are in agreement with Pradhan and Zhang's damped results [10], but the present undamped cross sections are much higher than those in Ref. [10] in the $(1s2p\ ^1P)3d\ ^2P$ resonance, at an energy of about 284.0 eV. The peak value is high by a factor of more than 1. This underestimate in Ref. [10] may be attributed to two factors: (1) the authors used the different method, and (2) their energy steps may not be close enough, as pointed out above. We employed fewer points to scan the energy region, and were able to repeat their results. In general, the narrow resonances are important contributors to radiation damping. Loose scanning cannot fully resolve such resonances; damping effects, therefore, are underestimated. But such underestimates do not have a serious influence on the damped cross sections in some cases, such as when the resonance is extremely narrow, as is readily seen from Eq. (11). In the perturbative calculation, we obtain similar results. However, the resonance positions are not precise, while the calculated resonance line profiles show good agreement. It should be mentioned that for the $(1s2p\ ^1P)3d\ ^2P$ resonance, we employed the energy level and autoionization width from accurate calculations using the saddle-point technique [38], instead of our values. This is because, for the weaker transitions, the treatment of electron correlation in Cowan's code is not reliable; our energy level is low by 0.8 eV and Γ_a is small by a factor of about 5, compared with those from the accurate saddle-point technique. At the last resonance, the good agreement with both the experiment and our close-coupling calculations in both the position and line profile demonstrated the success of the saddle-point technique. On the basis of the detailed calculation, at the peak we found that the unconvolved cross sections of this resonance are damped by a factor of up to more than 10. This can also easily be deduced from Eq. (11), and the given value 0.721 for the radiation branching ratio in Ref. [38]. Moreover, we note that the contributors to the experimental peak at energy 282.6 eV are not restricted to the labeled state $(1s2p\ ^1P)3p\ ^2S$ in Fig. 4 of Ref. [38]. In fact, another state $(1s2p\ ^1P)3d\ ^2F$ makes a more important contribution.

The photorecombination cross sections for the *KLN* resonance were evaluated and convolved with the experimental electron-energy distribution. They are displayed in Fig. 3(a) along with the experimental spectra [38]. A comparison with the theoretical results [10] was also made [see Figs. 3(a) and 3(b)]. The comparison showed that our damped results from the close-coupling *R*-matrix approach are better than Pradhan and Zhang's in both the resonance position and structure. Furthermore, we found that at energy about 294 eV the cross sections are damped by a factor of more than 3. This is different from Pradhan and Zhang's results. Their calculations in this energy region showed very small radiation damping effects. The cross sections in Ref. [10] were convoluted with a Gaussian function of FWHM 0.57 eV besides being calculated by different methods. But this does not cause the discrepancy in this energy region, due to the relation between and $T_\parallel$ and ΔE(FWHM). The reasons why the effects were underestimated in Pradhan and Zhang's investigation were analyzed above. In the calculation, we found it is a narrow resonance at near 294 eV that makes a significant contribution to damping. To display the influence of radiation damping on distinct resonances, we convoluted the cross

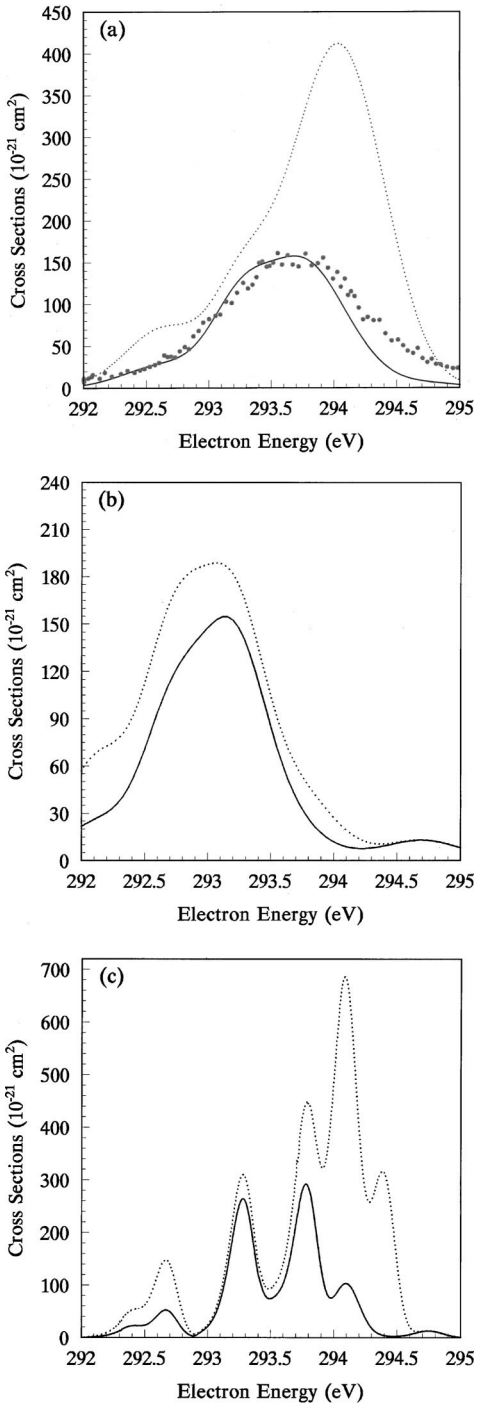

FIG. 3. (a) The same as in Fig. 1(b), but for the *KLN* resonance. (b) The same as in Fig. 1(c). (c) The convolved photorecombination cross sections with an artificial electron-energy distribution $T_\perp = 10^{-5}$ eV, where the solid and dotted curves represent the damped and undamped results, respectively.

sections with an artificial electron-energy distribution with a resolution higher than that of Mannervik *et al.*, say, $T_{\|} = 10^{-5}$ eV [Fig. 3(c)]. We saw very important influences on distinct resonances. A similar conclusion was also reported by Badnell, Gorczyca, and Price [18]. They calculated the cross sections for the *KLn* $(n=4-7)$ resonances in intermediate-coupling perturbative theory, *LS*-coupling perturbative theory, and *R*-matrix theory, and came to a consistent conclusion about radiation damping. We do not give perturbative results for the *KLN* resonance. This is because it is very difficult to evaluate this resonance accurately using the present perturbative code, since it includes weaker transitions than the *KLL* and *KLM* resonances. It is well known that many perturbative codes cannot give good results for weak transitions. For the present purpose, inaccurate positions and widths cannot give useful results.

IV. SUMMARY AND CONCLUSION

Within the framework of the rigorous continuum-bound transition of Davies and Seaton, we have developed a numerical method to calculate the low-lying resonance photorecombination by directly evaluating the Cauchy principal value of the integral in scattering matrices. This method turned out to be superior to the inverse-photoionization method [the dotted lines in Figs. 2(b) and 3(a)]. The latter greatly overestimates photorecombination for some resonances of C^{4+}, due to the neglect of radiative widths. Also, our method is superior to the parametrized method, in which the dipole matrix elements are expanded into an analytic expression and then the parameters in the expression are fitted, since the fitting is very difficult, and almost impossible for nonisolated resonances. Therefore, it is impracticable to employ the parametrized method to calculate photorecombination with stronger resonance-resonance interference. Our method, on the contrary, is naturally applicable to systems with stronger resonance-resonance interference. In such systems, standard perturbative theory is also invalid, because high-order interference effects cannot be fully taken into account. On the basis of this scheme, we calculated photorecombination for C^{4+} ions in the low-lying *KLL*, *KLM*, and *KLN* resonances. Comparisons of the present results with high-resolution experimental measurements and available theoretical calculations demonstrated the reliability of our method. The importance of radiation damping in the low-lying resonance photorecombination of C^{4+} was noted. Later, we will employ the method developed to study (1) the resonance-resonance interference in photorecombination of some systems, and (2) radiation damping effects in photorecombination of non-helium-like ions.

ACKNOWLEDGMENTS

We are grateful to Dr. S. Mannervik for providing us with his experimental data, and to Professor Pradhan and Dr. H. L. Zhang for sending us their theoretical data. One of us (L.B.Z.) is indebted to Dr. N. R. Badnell for some helpful communications.

[1] *Recombination of Atomic Ions*, Vol. 269 of *NATO Advanced Study Institute, Series B: Physics*, edited by W. G. Graham *et al.* (Plenum, New York, 1992).
[2] H. P. Summers, Adv. At., Mol., Opt. Phys. **33**, 275 (1994).
[3] H. E. Mason and B. C. Monsignori-Fossi, Astron. Astrophys. Rev. **6**, 123 (1992).
[4] J. Dubau and S. Volonte, Rep. Prog. Phys. **43**, 199 (1980).
[5] P. C. W. Davies and M. J. Seaton, J. Phys. B **2**, 757 (1969).
[6] L. H. Andersen, Comments At. Mol. Phys. **27**, 25 (1991).
[7] R. H. Bell and M. J. Seaton, J. Phys. B **18**, 1589 (1985); A. K. Pradhan and M. J. Seaton, *ibid.* **18**, 1631 (1985).
[8] S. N. Nahar and A. K. Pradhan, Phys. Rev. Lett. **68**, 1488 (1992); Phys. Rev. A **49**, 1816 (1994).
[9] F. Robicheaux, T. W. Gorczyca, M. S. Pindzola, and N. R. Badnell, Phys. Rev. A **52**, 1319 (1995).
[10] A. K. Pradhan and H. L. Zhang, J. Phys. B **30**, L571 (1997); H. L. Zhang and A. K. Pradhan, *ibid.* **31**, 1459 (1999).
[11] J. G. Wang, T. Kato, and I. Murakami, Phys. Rev. A **60**, 3750 (1999).
[12] Y. Zou, L. B. Zhao, and Q. Y. Fang, Phys. Rev. A **60**, 4510 (1999).
[13] L. H. Andersen, P. Hvelplund, H. Hundsen, and P. Kvistgaad, Phys. Rev. Lett. **62**, 2656 (1989).
[14] L. H. Andersen, J. Bolko, and P. Kvistgaad, Phys. Rev. A **41**, 1293 (1990).
[15] D. R. DeWitt, E. Lindroth, R. Schuch, H. Gao, T. Quinteros, and W. Zong, J. Phys. B **28**, L147 (1995).
[16] D. A. Knapp, P. Beiersdorfer, M. H. Chen, J. H. Scofield, and Schneider, Phys. Rev. Lett. **74**, 54 (1995).
[17] T. W. Gorczyca and N. R. Badnell, Phys. Rev. Lett. **79**, 2783 (1997); J. Phys. B **29**, L283 (1996).
[18] N. R. Badnell, T. W. Gorczyca, and A. D. Price, J. Phys. B **31**, L239 (1998).
[19] L. H. Andersen, G. Y. Pan, T. Shmidt, N. R. Badnell, and M. S. Pindzola, Phys. Rev. A **45**, 7868 (1992).
[20] N. R. Badnell, M. S. Pindzola, and D. C. Griffin, Phys. Rev. A **41**, 2422 (1990).
[21] L. B. Zhao (unpublished).
[22] S. Schennach, A. Muller, O. Uwira, J. Haselbauer, W. Spies, A. Frank, M. Wagner, R. Backer, M. Kleinod, E. Jennewein, N. Angert, P. H. Mokler, N. R. Badnell, and M. S. Pindzola, Z. Phys. D: At., Mol. Clusters **30**, 291 (1994).
[23] H. Gao, D. R. DeWitt, R. Schuch, W. Zong, S. Asp, and M. Pajek, Phys. Rev. Lett. **75**, 4381 (1995).
[24] H. Gao, R. Schuch, W. Zong, E. Justiniano, D. R. DeWitt, H. Lebius, and W. Spies, J. Phys. B **30**, L499 (1997).
[25] S. Schippers, T. Bartsch, C. Brandau, G. Gwinner, J. Linkemann, A. Muller, A. A. Saghiri, and A. Wolf, J. Phys. B **31**, 4873 (1998); Phys. Rev. A **59**, 3092 (1999).
[26] T. W. Gorczyca, M. S. Pindzola, F. Robicheaux, and N. R. Badnell, Phys. Rev. A **56**, 4742 (1997).
[27] S. Schippers, T. Bartsch, C. Brandau, G. Gwinner, J. Linke-

mann, A. Muller, A. A. Saghiri, and A. Wolf, in *Proceedings of the XXI ICPEAC, Sendai, Japan, 1999, Abstracts of Contributed Papers*, edited by Y. Itikawa *et al.* (University of Electro-Communications, Tokyo, 1999), p. 385.
[28] L. B. Zhao and S. C. Li, Phys. Rev. A **55**, 1039 (1997).
[29] T. W. Gorczyca, F. Robicheaux, M. S. Pindzola, and N. R. Badnell, Phys. Rev. A **54**, 2107 (1996).
[30] M. S. Pindzola, F. Robicheaux, N. R. Badnell, M. H. Chen, and M. Zimmermann, Phys. Rev. A **52**, 420 (1995).
[31] P. G. Burke, A. Hibbert, and W. D. Robb, J. Phys. B **4**, 153 (1971); Adv. At. Mol. Phys. **11**, 143 (1975).
[32] K. Sakimoto, M. Terao, and K. A. Berrington, Phys. Rev. A **42**, 291 (1990).
[33] D. G. Griffin, M. S. Pindzola, F. Robicheaux, T. W. Gorczyca, and N. R. Badnell, Phys. Rev. Lett. **72**, 3491 (1994).
[34] K. Sakimoto, J. Phys. B **24**, 3049 (1991).
[35] K. A. Berrington, W. B. Eissner, and P. H. Norrington, Comput. Phys. Commun. **92**, 290 (1995).
[36] A. Hibbert, Comput. Phys. Commun. **9**, 141 (1975).
[37] E. Clementi and C. Roetii, At. Data Nucl. Data Tables **14**, 177 (1974).
[38] S. Mannervik, S. Asp, L. Brostrom, D. Dewitt, J. Lidberg, R. Schuch, and K. T. Chung, Phys. Rev. A **55**, 1810 (1997).
[39] R. D. Cowan, *The Theory of Atomic Structure and Spectra* (University of California Press, Berkeley, CA, 1981).
[40] Y. M. Li, Y. Zou, and L. B. Zhao, in *Proceedings of the XVI International Conference on Atomic Physics, Windsor, Canada, 1998*, edited by W. E. Baylis and G. W. F. Drake, AIP Conf. Proc. No. 477 (AIP, Woodbury, NY, 1999), p. 481.
[41] A. Ichihara and J. Eichler, At. Data Nucl. Data Tables (to be published).